Gong, Hanyang; Polojärvi, Arttu; Tuhkuri, Jukka

# 3D DEM study on the effect of ridge keel width on rubble resistance on ships

*Published in:*
ASME 2018 37th International Conference on Ocean, Offshore and Arctic Engineering

*DOI:*
10.1115/OMAE2018-78765

Published: 17/06/2018

*Document Version*
Publisher's PDF, also known as Version of record

**Proceedings of the ASME 2018 37th International Conference on Ocean, Offshore and Arctic Engineering OMAE2018 June 17-22, 2018, Madrid, Spain**

**OMAE2018-78765**

# 3D DEM STUDY ON THE EFFECT OF RIDGE KEEL WIDTH ON RUBBLE RESISTANCE ON SHIPS

**Hanyang Gong***
Department of Mechanical Engineering
Aalto University
Espoo 02150
Finland
Email: hanyang.gong@aalto.fi

**Arttu Polojärvi**
Department of Mechanical Engineering
Aalto University
Espoo 02150
Finland
Email: arttu.polojarvi@aalto.fi

**Jukka Tuhkuri**
Department of Mechanical Engineering
Aalto University
Espoo 02150
Finland
Email: jukka.tuhkuri@aalto.fi

## ABSTRACT

*In this paper, we use 3D discrete element method (DEM) to simulate ship penetration through a non-cohesive rubble pile presenting a ridge keel. We study the effect of the pile width on the rubble resistance and the relation between the resistance records and rubble deformation. The peak rubble resistance increases with the rubble pile width, but the rate of the increase is not constant. The peak rubble resistance values from the simulations with the widest rubble piles are compared to the ones yielded by the analytical models with success.*

## INTRODUCTION

Ice ridges are commonly encountered by ships on ice-covered seas. Due to this, the ridge resistance on ships has a central role in route planning and optimization of marine transport. Ridge resistance is usually divided into components related to the structure of a ridge: keel (an underwater pile of loose or partly cohesive ice rubble), consolidated layer (refrozen layer close to the water line), and sail (rubble pile above water line) [1]. The resistance of the consolidated layer is sometimes assumed approximately equal to that of the level ice [2] and sail resistance insignificant and therefore often not considered. This paper focuses on a keel resistance by studying the resistance of ice rubble pile on a ship.

Rubble resistance has been studied using various approaches including experiments and analytical and numerical models. In analytical approaches on ridge resistance, rubble piles are generally assumed to have a geometry of a semi-infinite rubble field, with an infinite width and a finite depth [3, 4]. In these approaches, the rubble is assumed to follow Mohr-Coulomb type of material behavior. Somewhat similar analytical approaches have been used in ridge-structure interaction analyses [5, 6]. Croasdale [6] estimated ridge loads on a sloping structure with a composite beam model, which accounted for the ridge width and included the consolidated layer. Numerical modeling of ice rubble has been performed using continuum models [7–9] and discrete element method (DEM) [10–16].

This paper presents our study on ice rubble resistance using DEM simulations. First, we introduce the simulation set up. Then we present our results on the rubble resistance records and analyze them using snapshots from the simulations. After this, we discuss the effect of pile width on peak rubble resistance, and compare our results to analytical models, before we conclude our paper.

## SIMULATION SET UP

Simulations were done using an in-house 3D DEM code of Aalto University Ice Mechanics Group. This code has been validated by modeling ridge keel punch through tests [13, 14] and it has been used to simulate ship penetration through a ridge keel [17]. The simulations are explicit and we model the ship

*Address all correspondence to this author.

 

**TABLE 1.** THE MAIN PARAMETERS USED IN SIMULATIONS.

| | Parameter | Unit | Value |
|---|---|---|---|
| General | Gravitational acceler. | $m/s^2$ | 9.81 |
| | Time interval | s | 5 |
| Contact | Penalty term | - | $1 \cdot 10^7$ |
| | Damping constant | - | $5 \cdot 10^5$ |
| | Time step | s | $5 \cdot 10^{-5}$ |
| Ice blocks | Thickness | m | 0.3 |
| | Block aspect ratio | - | 0.6 ... 15 |
| | Ice-ice friction coef. $\mu_i$ | - | 0.3, 0.6 |
| | Mass density $\rho_i$ | $kg/m^3$ | 920 |
| Water | Mass density $\rho_w$ | $kg/m^3$ | 1010 |
| Rubble* | Width $w$ | m | 17.3...160 |
| | Depth $h$ | m | 5 |
| | Keel angle | $^\circ$ | 30 |
| | Porosity $p$ | | 0.4 |
| Ship | Waterline length | m | 150 |
| | Midbody length $L_m$ | m | 67.5 |
| | Breadth $B$ | m | 22.2 |
| | Draft $T$ | m | 9.5 |
| | Bow length $L_{bow}$ | m | 40 |
| | Waterline half-angle $\alpha$ | $^\circ$ | 25.2 |
| | Stem angle $\varphi$ | $^\circ$ | 29.7 |
| | Ship-ice friction coef. $\mu_s$ | - | 0.1 |
| | Ship velocity | $m/s$ | 1 |

*values refer to the initial pile geometry.

and the ice blocks of the rubble as polyhedral rigid bodies. The ship-to-block and block-to-block contacts yield contact forces, which compose of elastic and viscous damping forces in normal direction and of frictional force in tangential direction. Additionally, buoyant, gravitational and drag forces act on ice blocks in the simulation. Table 1 shows the simulation parameters.

Fig. 1 presents the simulation basin with the coordinate system used in this paper. The basin extended far enough into the $x$- and $z$-directions to keep any of the blocks, or the ship, from interacting with the basin walls in these directions. The center line of the ship was parallel to the $x$-axis and aligned with the center

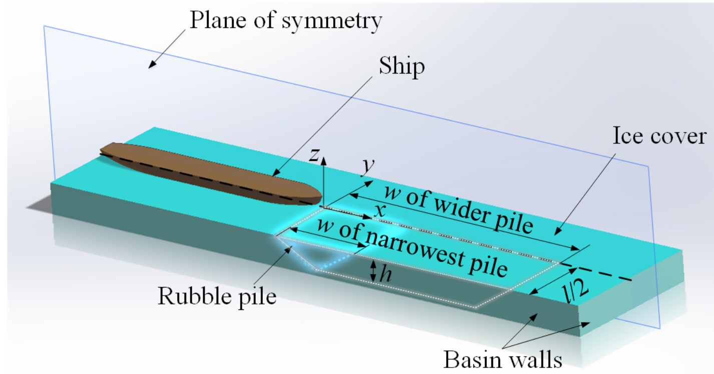


**FIGURE 1.** A SKETCH OF THE SIMULATION BASIN AND THE COORDINATE SYSTEM USED IN THIS PAPER. THE NARROWEST PILE HAD A TRIANGULAR CROSS-SECTION (BLUE LINES) WHEREAS THE WIDER PILES HAD A TRAPEZOIDAL CROSS-SECTION (GRAY LINES). THE SHIP MOVED INTO THE POSITIVE $x$-DIRECTION.

line of the basin. The model has a plane of symmetry on $xz$-plane and we could use a half model in our simulations (rigid wall at $y = 0$ m and rubble in the half domain $-30$ m $< y < 0$ m only) as described in [17]. The whole basin was covered by a rigid plate mimicking the ice cover on top of the ice rubble.

Before initializing the rubble pile, the shapes of the blocks had to be generated. All blocks had a fixed thickness, while their width and length were randomly chosen using a block aspect ratio distribution measured from full-scale ridge sails [18]. The ice rubble was then generated by releasing the blocks underwater, and by letting the simulation run until the drag, the viscous damping and the frictional forces had dissipated the kinetic energy of the blocks [13].

After the rubble mass had become to rest, the blocks that did not belong to the wanted pile geometry were removed from the simulation. We tested pile widths $w = 17.3 \ldots 160$ m (into the $x$-direction) and ran simulations with two different ice-ice friction coefficient $\mu_i$ values. The narrowest pile had a triangular cross-section, while the cross-section of the wider piles was trapezoidal (see the shapes illustrated in Fig. 1). All piles had the depth $h$ of 5 m and the keel angle of 30°. The basin cover provided frictional resistance on the rubble pile so that it would not dissolve.

The generated rubble pile was used as an input for the simulations of the actual ship-pile interaction. In these simulations, the ship moved with a constant velocity into the positive $x$-direction and penetrated the rubble pile. The ship geometry was chosen after M/T Uikku with its dimensions given in Fig. 2. The basin cover did not interact with the ship (no contact forces between the ship and the cover) nor did the cover fracture. Hence, the cover provided just the aforementioned frictional resistance

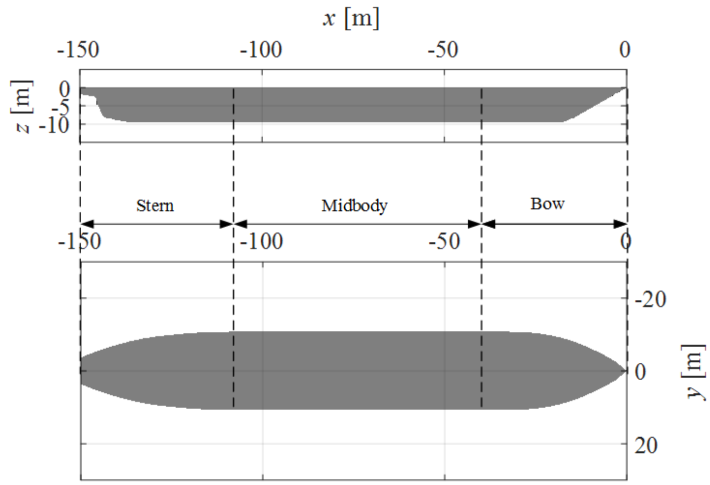


**FIGURE 2**. DIMENSIONS OF M/T UIKKU USED IN THE SIMULATIONS.

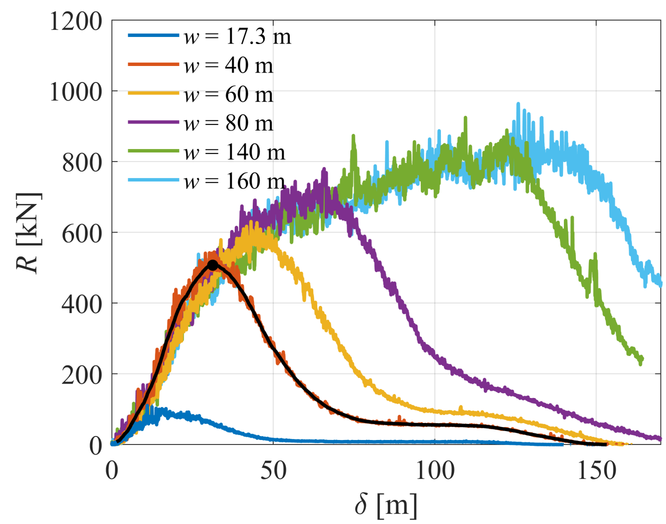


**FIGURE 3**. THE RUBBLE RESISTANCE-PENETRATION ($R-\delta$) RECORDS FROM THE SIMULATIONS WITH DIFFERENT RUBBLE PILE WIDTHS $w$. THE BLACK LINE ON TOP OF THE $w = 40$ m DATA SHOWS AN EXAMPLE OF THE FILTERED DATA, WHICH WAS USED TO DEFINE PEAK RESISTANCE $R^{\mathrm{p}}$ (BLACK MARKER) VALUE.

for the rubble pile. The rubble resistance $R$ was recorded on each simulation time step. As the ship moved into the positive $x$-direction, $R$ was defined to be equal to the negative $x$-component of the load applied by the rubble on the ship hull.

## RESULTS AND ANALYSIS

This section first introduces the ridge resistance records yielded by our simulations. Then it presents an analysis on the relation between the rubble pile deformation and the rubble resistance records.

### The Rubble Resistance Records

Fig. 3 shows the rubble resistance-penetration ($R-\delta$) records from our simulations with all six pile widths $w$ used. These simulations were run with ice-ice friction coefficient $\mu_{\mathrm{i}} = 0.3$. The noise in the $R-\delta$ records is due to the individual ice blocks within the rubble, which had a random initial configuration, impacting the ship hull. The general features of $R-\delta$ records are similar for all simulated cases: load increases, reaches it maximum value that depends on $w$, and then decreases. For piles with $w > 60$ m, the rate of increasing resistance, $\partial R/\partial\delta$, drops at around $\delta = 50$ m. Increasing the friction coefficient from $\mu_{\mathrm{i}} = 0.3$ to $\mu_{\mathrm{i}} = 0.6$ did not affect the general features of the $R-\delta$ records.

Fig. 3 further indicates the peak value $R^{\mathrm{p}}$ of the rubble resistance for the case $w = 40$ m with a marker. The peak value $R^{\mathrm{p}}$ was defined as illustrated in the figure: $R^{\mathrm{p}}$ was the maximum of the running average on the corresponding data. The running average enabled us to study the general trends in peak resistance as it filtered out the configuration-depended noise in the resistance records. The window size for the running average was 6 m. As the figure shows, the general features of the $R-\delta$ records preserved well when the running average with this window size was used and, thus, the $R^{\mathrm{p}}$ defined using the running average is representative for the data.

### Resistance of the narrow piles

Fig. 4 presents the $R-\delta$ for the narrowest pile, which had width $w = 17.3$ m and a triangular profile. In addition, the figure shows three markers ①-③. These markers refer to the three snapshots taken from the same simulation and presented in Fig. 5. By comparing the $R-\delta$ graph and the snapshot at ①, it can be seen that $R^{\mathrm{p}}$ is reached close to the instance the ship bow has reached the deepest part of the rubble pile. At ② the pile has started to widen due to its deformation, and the load drops, as the pile dissolves towards the positive $x$-direction. The residual load at ③ is due to the friction of the rubble mass acting on the midbody of the ship when the ship travels through the pile.

### Resistance of the wide piles

The interaction between the ship and a wide rubble pile differs from that described above. The process is described by Figs. 6 and 7. Fig. 6 presents the $R-\delta$ for the widest pile having width $w = 160$ m and a trapezoidal profile. Again, the figure

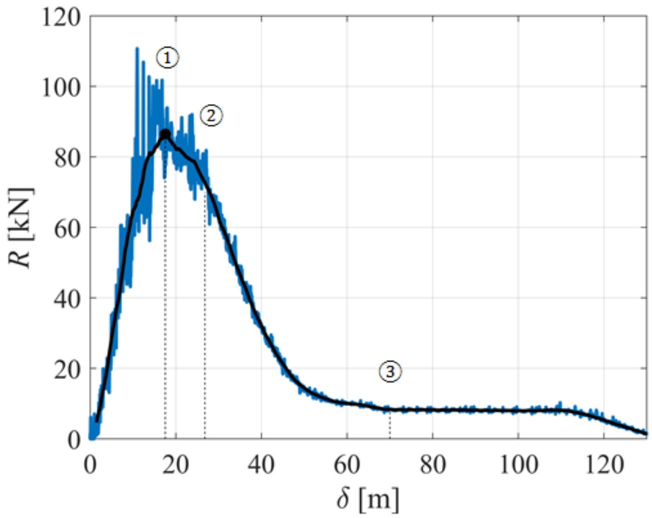


**FIGURE 4**. THE RESISTANCE RECORD FOR RUBBLE PILE HAVING WIDTH $w = 17.3$ m AND FRICTION COEFFICIENT $\mu_\mathrm{i}$ = 0.3. FIGURE ALSO SHOWS THE FILTERED DATA (BLACK LINE) AND THE PEAK RESISTANCE VALUE $R^\mathrm{p}$ (BLACK MARKER). MARKERS ①-③ REFER TO SNAPSHOTS OF FIG. 5

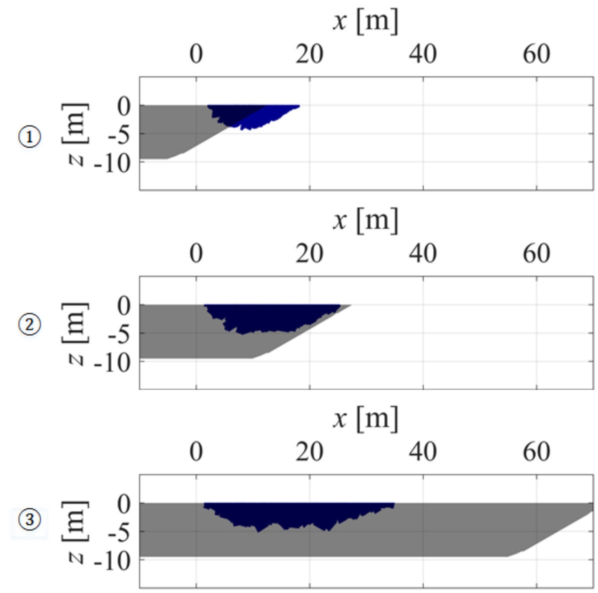


**FIGURE 5**. THE SNAPSHOTS OF SHIP-PILE PENETRATION PROCESS FOR RUBBLE PILE WITH $w = 17.3$ m. THE RESISTANCE-PENETRATION CURVE FOR THIS SIMULATION IS GIVEN IN FIGURE 4. THE FIGURE ONLY SHOWS THE UNDERWATER PART OF THE SHIP HULL.

shows the three markers ①-③. The markers refer to the three snapshots of Fig. 7. Fig. 6 shows that the load initially increases with high rate $\partial R/\partial \delta$ up to ①. Fig. 7 shows, that ① is the instance the ship bow has just totally penetrated into the deepest part of the rubble pile, and that the rubble blocks have been forced to move downwards (and away from the ship center line). The rate of increase $\partial R/\partial \delta$ is about equal for the narrow and wide pile up to ① (see Figs. 3, 4 and 6).

Between ① and ② of Figs. 6 and 7, the ship keeps on penetrating further into the rubble pile, and the load gradually increases towards $R^\mathrm{p}$. During the penetration interval between ① and ②, there is virtually no rubble motion on the side of the midbody of the ship, but instead, the rubble appears to be in a static equilibrium. After $R^\mathrm{p}$ is reached at ②, the load starts to decrease. As seen from the snapshot ③ of Fig. 7, this is due to the pile dissolving towards the positive $x$-direction.

### The Effect of Pile Width on Peak Resistance

Fig. 8 shows the $R^\mathrm{p}$ values yielded by the simulations plotted against the pile width $w$ with both friction coefficient $\mu_\mathrm{i}$ values used. The effect of $w$ on $R^\mathrm{p}$ is drastic, as $R^\mathrm{p}$ shows up to ninefold increase for the range of $w$ values used (17.32...160 m). It is interesting to notice, that the $R^\mathrm{p} - w$ data of Fig. 8 shows two distinct regimes. When $w < 40$ m, $R^\mathrm{p}$ shows a stronger dependency on $w$ than with $w > 40$ m. $R^\mathrm{p}$ appears to be equal for $w = 140$ m and $w = 160$ m. Friction coefficient $\mu_\mathrm{i}$ has a clear, but less pronounced effect on $R^\mathrm{p}$ values. Increasing $\mu_\mathrm{i}$ from 0.3 to 0.6 increased $R^\mathrm{p}$ by about 10-90 % depending on $w$. The effect of $\mu_\mathrm{i}$ was strongest with low $w$ and then got weaker as $w$ increased. The study on the reasons behind these results is out of the scope of this paper.

## DISCUSSION

We compared our results to an analytical model presented by Malmberg [4], which is recommended by a report for Finnish-Swedish ice class rules [19]. The formula reads (see Table 1 for most of the symbols)

$$\begin{aligned} R_\mathrm{A} =& C_1 T h \left(\frac{B}{2} + h\tan\psi\cos\alpha\right)(\mu_\mathrm{s}\cos\alpha + \sin\psi\sin\alpha) + \\ & C_2 T L_\mathrm{m}\left[K_0 h + \left(\frac{h}{T} - \frac{1}{2}\right)B\right], \end{aligned} \tag{1}$$

where the constants $C_1$ and $C_2$ are

$$\begin{aligned} C_1 &= (1-p)(\rho_\mathrm{w} - \rho_\mathrm{i}) g K_\mathrm{p} \\ C_2 &= (1-p)(\rho_\mathrm{w} - \rho_\mathrm{i}) g \mu_\mathrm{s}. \end{aligned} \tag{2}$$

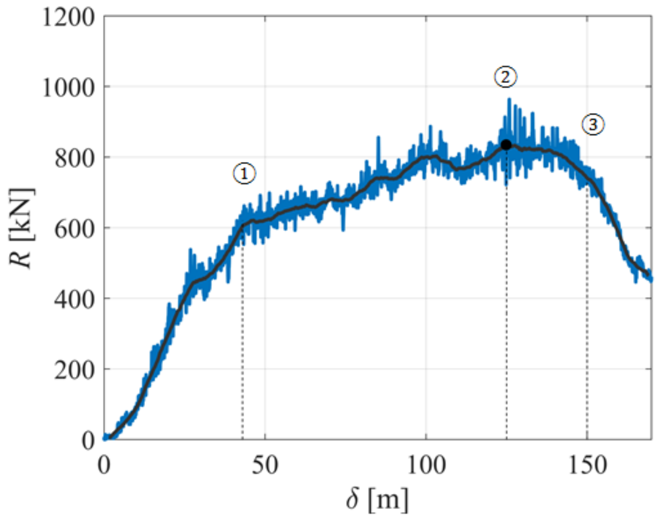


**FIGURE 6**. THE RESISTANCE RECORD FOR RUBBLE PILE HAVING WIDTH $w = 160$ m AND FRICTION COEFFICIENT $\mu_\mathrm{i} = 0.3$. FIGURE ALSO SHOWS THE FILTERED DATA (BLACK LINE) AND THE PEAK RESISTANCE VALUE $R^\mathrm{p}$ (BLACK MARKER). MARKERS ①-③ REFER TO SNAPSHOTS OF FIG. 7

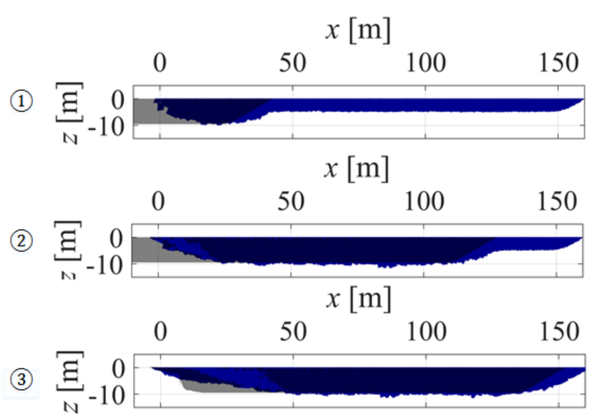


**FIGURE 7**. THE SNAPSHOTS OF SHIP-PILE PENETRATION PROCESS FOR RUBBLE PILE WITH $w = 160$ m. THE RESISTANCE-PENETRATION CURVE FOR THIS SIMULATION IS GIVEN IN FIG. 6. THE FIGURE ONLY SHOWS THE UNDERWATER PART OF THE SHIP HULL.

In these equations the parameters related to the ship hull geometry are the ship breadth $B$, draft $T$, midbody length $L_\mathrm{m}$, stem angle $\varphi$, waterline half-angle $\alpha$, and flare angle $\psi = \arctan(\tan\varphi/\sin\alpha)$. The rubble material properties, on the other hand, include the internal friction angle $\phi$, porosity $p$, ship-ice friction coefficient $\mu_\mathrm{s}$, water density $\rho_\mathrm{w}$ and ice density $\rho_\mathrm{i}$, and

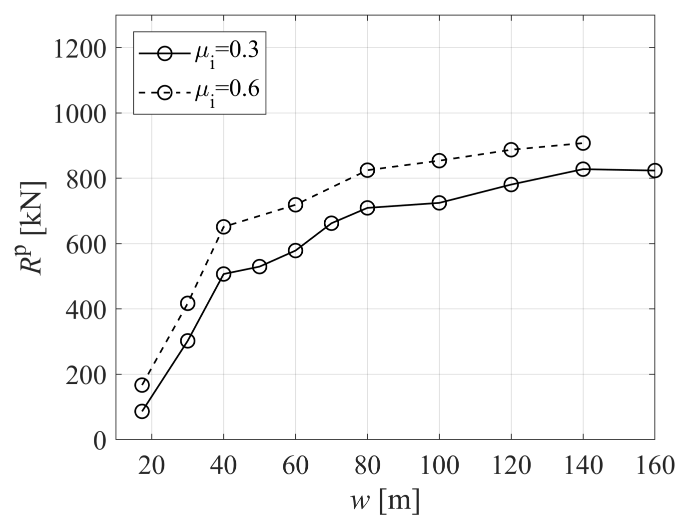


**FIGURE 8**. THE PEAK RESISTANCE-PILE WIDTH ($R^\mathrm{p} - w$) RECORDS FROM THE SIMULATIONS FOR THE TWO ICE-ICE FRICTION COEFFICIENT $\mu_\mathrm{i}$ VALUES USED.

the parameters related to rubble pile failure criterion are the coefficient of active pressure at rest $K_0$ (0.27) [19] and the coefficient of passive pressure $K_\mathrm{p} = \tan^2(45+\phi/2)$. $K_0$ describes the ratio of pressure to rubble weight, when the rubble pile acting on the ship hull is in a state of static equilibrium, while $K_\mathrm{p}$ describes the rubble pressure, when the ship hull pushes against the rubble and displaces it. Other parameters include pile depth $h$ and gravitational acceleration $g$. It can be noticed, that the pile width $w$ is not considered by Eqn. (1).

With the dimensions and the parameters of our simulations, the resistance $R_\mathrm{A}$ given by Eqn. (1) is about 900 kN, when we set $\phi = 40°$ and $p = 0.4$. The chosen $\phi$ value is typical for ice rubble [18], while we measured porosity $p \approx 0.4$ for the simulated rubble. Peak resistance $R^\mathrm{p}$ in our simulations with the pile width $w \geq 140$ m was about 800-900 kN (see Fig. 8). Thus the peak resistance for the widest rubble piles in our simulations compare very well with the $R_\mathrm{A}$ value given by Eqn. (1).

## CONCLUSIONS

In this study, we simulated the ship-pile interaction process using 3D DEM. We presented the rubble resistance $R$-records for narrow and wide ridge keels, and showed that $R$ depends on $w$. The $R$-records for the wide piles show two different regimes: first $R$ increases fast, then slower. We found that the peak resistance $R^\mathrm{p}$ depends on pile width $w$. These finding could have implications on, for example, marine traffic route optimization and transit simulations.

## ACKNOWLEDGMENT

We are grateful for the support from the Academy of Finland through the project Kara-Arctic Monitoring and Operation Planning Platform (KAMON).

## REFERENCES

[1] Timco, G., and Burden, R., 1997. "An analysis of the shapes of sea ice ridges". *Cold regions science and technology,* ***25***(1), pp. 65–77.

[2] Riska, K., 2014. Factors influencing the power requirement in the finnish-swedish ice class rules. Tech. Rep. 67, Finnish Maritime Administration, Winter Navigation Research Board.

[3] Keinonen, A., 1979. "An analytical method for calculating the pure ridge resistance encountered by ships in first year ice ridges". PhD thesis, Teknillinen Korkeakoulu.

[4] Malmberg, S., 1983. "Om fartygs fastkilning i is". Master's thesis, Helsinki University of Technology.

[5] Dolgopolov, Y., Afanasiev, V., Koren'Kov, V., and Panfilov, D., 1975. "Effect of hummocked ice on the piers of marine hydraulic structures". In International Symposium on Ice Problems, 3rd, Proceedings, Dartmouth College, Hanover, NH. Aug., 18-21. 1975.

[6] Croasdale, K., and Cammaert, A., 1994. "An improved method for the calculation of ice loads on sloping structures in first-year ice". *Power Technology and Engineering (formerly Hydrotechnical Construction),* ***28***(3), pp. 174–179.

[7] Heinonen, J., 2004. "Constitutive modeling of ice rubble in first-year ridge keel". PhD thesis, Helsinki University of Technology.

[8] Serré, N., 2011. "Mechanical properties of model ice ridge keels". *Cold Regions Science and Technology,* ***67***(3), pp. 89–106.

[9] Serré, N., 2011. "Numerical modelling of ice ridge keel action on subsea structures". *Cold Regions Science and Technology,* ***67***(3), pp. 107–119.

[10] Hopkins, M. A., 1992. Numerical simulation of systems of multitudinous polygonal blocks. Tech. rep., DTIC Document.

[11] Hopkins, M. A., 1998. "Four stages of pressure ridging". *Journal of Geophysical Research: Oceans,* ***103***(C10), pp. 21883–21891.

[12] Hopkins, M. A., Hibler, W., and Flato, G., 1991. "On the numerical simulation of the sea ice ridging process". *Journal of Geophysical Research: Oceans,* ***96***(C3), pp. 4809–4820.

[13] Polojärvi, A., and Tuhkuri, J., 2009. "3D discrete numerical modelling of ridge keel punch through tests". *Cold Regions Science and Technology,* ***56***(1), pp. 18–29.

[14] Polojärvi, A., and Tuhkuri, J., 2012. "Velocity effects in laboratory scale punch through experiments". *Cold Regions Science and Technology,* ***70***, pp. 81–93.

[15] Polojärvi, A., Tuhkuri, J., and Korkalo, O., 2012. "Comparison and analysis of experimental and virtual laboratory scale punch through tests". *Cold Regions Science and Technology,* ***81***, pp. 11–25.

[16] Hisette, Q., Alekseev, A., Seidel, J., et al., 2017. "Discrete element simulation of ship breaking through ice ridges". In The 27th International Ocean and Polar Engineering Conference, International Society of Offshore and Polar Engineers.

[17] Gong, H., Polojrvi, A., and Tuhkuri, J., 2017. "Preliminary 3D DEM simulations on ridge keel resistance on ships". In The 24th International Conference on Port and Ocean Engineering under Arctic Conditions, International Society of Offshore and Polar Engineers.

[18] Kulyakhtin, S., and Høyland, K. V., 2014. "Study of the volumetric behaviour of ice rubble based on bi-axial compression data". In ASME 2014 33rd International Conference on Ocean, Offshore and Arctic Engineering, American Society of Mechanical Engineers, pp. V010T07A027–V010T07A027.

[19] Riska, K., Max, W., and Kim, E., 1997. Performance of merchant vessels in ice in the baltic. Tech. Rep. 52, Finnish Maritime Administration, Winter Navigation Research Board.

 